Title

Perinatal exposure to nicotine alters spermatozoal DNA methylation near genes controlling nicotine action

Journal

The FASEB Journal, 35(7)

ISSN

0892-6638

Authors

Altıntaş, Ali
Liu, Jie
Fabre, Odile
et al.

Publication Date

2021-07-01

DOI

10.1096/fj.202100215r

Peer reviewed

Published in final edited form as:

FASEB J. 2021 July ; 35(7): e21702. doi:10.1096/fj.202100215R.

Perinatal exposure to nicotine alters spermatozoal DNA methylation near genes controlling nicotine action

Ali Altintaş[1],

Jie Liu[2],

Odile Fabre[1],

Tsai-Der Chuang[2],

Ying Wang[2],

Reiko Sakurai[2],

Galal Nazih Chehabi[1],

Romain Barrès[1],

Virender K. Rehan[2]

[1]Novo Nordisk Foundation Center for Basic Metabolic Research, University of Copenhagen, Copenhagen, Denmark

[2]Lundquist Institute for Biomedical Innovation at Harbor-ULCA Medical Center, David Geffen School of Medicine at UCLA, Torrance, CA, USA

Abstract

Perinatal smoke/nicotine exposure alters lung development and causes asthma in exposed offspring, transmitted transgenerationally. The mechanism underlying the transgenerational inheritance of perinatal smoke/nicotine-induced asthma remains unknown, but germline epigenetic modulations may play a role. Using a well-established rat model of perinatal nicotine-induced asthma, we determined the DNA methylation pattern of spermatozoa of F1 rats exposed perinatally to nicotine in F0 gestation. To identify differentially methylated regions (DMRs), reduced representation bisulfite sequencing was performed on spermatozoa of F1 litters. The top regulated gene body and promoter DMRs were tested for lung gene expression levels, and key proteins involved in lung development and repair were determined. The overall CpG methylation in F1 sperms across gene bodies, promoters, 5′-UTRs, exons, introns, and 3′-UTRs was not affected by nicotine exposure. However, the methylation levels were different between

Correspondence: Virender K. Rehan, Department of Pediatrics, The Lundquist Institute for Biomedical Innovation at Harbor UCLA Medical Center, David Geffen School of Medicine at UCLA, 1124 West Carson Street, Torrance, CA 90502, USA. vrehan@lundquist.org.

Ali Altintaş is first author.

Romain Barrès and Virender K. Rehan are shared last authors.

AUTHOR CONTRIBUTIONS

Study design: V.K. Rehan; conceptualization: V.K. Rehan, A. Altintaş, R. Barrès, J. Liu; sample preparation: J. Liu, O. Fabre, T.-D. Chuang, Y. Wang, R. Sakurai; bioinformatics analysis: A. Altintaş, G.N. Chehabi; manuscript: A. Altintaş, R. Barrès, V.K. Rehan, J. Liu.

CONFLICT OF INTEREST

The authors declare that they have no conflict of interest.

SUPPORTING INFORMATION

Additional Supporting Information may be found online in the Supporting Information section.

the different genomic regions. Eighty one CpG sites, 16 gene bodies, and 3 promoter regions were differentially methylated. Gene enrichment analysis of DMRs revealed pathways involved in oxidative stress, nicotine response, alveolar and brain development, and cellular signaling. Among the DMRs, *Dio1* and *Nmu* were the most hypermethylated and hypomethylated genes, respectively. Gene expression analysis showed that the mRNA expression and DNA methylation were incongruous. Key proteins involved in lung development and repair were significantly different (FDR < 0.05) between the nicotine and placebo-treated groups. Our data show that DNA methylation is remodeled in offspring spermatozoa upon perinatal nicotine exposure. These epigenetic alterations may play a role in transgenerational inheritance of perinatal smoke/nicotine induced asthma.

Keywords

DNA methylation; epigenetic inheritance; lung development; smoking; spermatozoa

1 | INTRODUCTION

Active or passive exposure of the developing offspring to cigarette smoke results in a lifelong decrease in offspring pulmonary function, increased risk of asthma, and chronic lung disease, even when the offspring do not smoke.[1–5] These effects of perinatal smoke exposure, traditionally attributed to the direct effects of smoke constituents on the developing lung, have been a cause of concern for decades. However, our recent demonstration that such effects are transmitted across generations[6,7] has greatly added to the significance of the consequences of smoke exposure to the developing fetus. This is particularly relevant since the erroneous perception that electronic cigarettes are safer than traditional cigarettes has led to a sharp increase in their use among women of reproductive age.[8–11] This adds to the importance of addressing the consequences of perinatal smoke exposure not only from the basic science perspective but also from a public health perspective. However, the mechanism underlying the transmission of perinatal smoke-induced lung phenotype across generations remains unknown.

Research using human cohorts with and without gestational smoke exposures across generations is required to determine the intergenerational and transgenerational effects in patients with asthma. Given the logistic limitations to study any human cohort across generations, particularly from a mechanistic perspective, animal models are used instead. Several animal models have been employed to study the effects of smoke exposure on developing lungs.[1,3,12–14] Although there are thousands of chemicals in cigarette smoke,[15] compelling evidence supports that most effects of perinatal smoke exposure on the developing lung, including the intergenerational and transgenerational transmission of the asthmatic phenotype, are caused by nicotine.[6,7,16] Specifically, the experimental asthmatic phenotype seen following perinatal nicotine exposure in the rat model used in this study and many other animal models is similar to that seen in human infants exposed perinatally to maternal smoke.[1,12–14,16] Therefore, perinatal nicotine exposure is a relevant model to study the effects of smoke exposure on the developing lung, including the transmission of the asthmatic phenotype across generations.

DNA methylation is one of the most studied and well-characterized epigenetic mark. Specifically, the cytosine residues located within cytosine and guanine dinucleotides can be dynamically methylated and demethylated by the activity of DNA methyltransferases (DNMTs) and ten-eleven translocation (TET) enzymes, respectively.[17] Maternal exposure to nicotine and tobacco smoking alters the DNA methylation signature in placental and offspring's somatic tissues.[18–20] This may be explained by direct exposure to nicotine, since nicotine can cross the placenta, and fetal concentration can be 15% higher than the maternal concentration.[19,21] Whether nicotine can affect the gametic epigenome of the developing offspring remains unknown.

Although the direct effects of smoke/nicotine exposure on the developing lung can mechanistically explain the pulmonary phenotype seen in F1 offspring, this does not explain the pulmonary effects seen in the subsequent non-exposed F2 and F3 offspring. Transmission of the environmentally induced phenotypes is likely mediated via germ cell epigenetic modifications. Epigenetic marks regulate transcriptional processes in both somatic and germ cell development and are carried from one cell division to the next, characterized as epigenetic programming.[22] We hypothesize that perinatal nicotine exposure alters the epigenetic machinery in germ cells leading to generationally heritable asthma phenotype. Previously we showed that global DNA-methylation was higher in the testes of F1 animals subjected to perinatal exposure to nicotine.[6,7,23] To investigate possible DNA methylation changes with a higher resolution, we profiled the genome-wide DNA methylation of spermatozoa from F1 male offspring exposed perinatally to nicotine using reduced representation bisulfite sequencing (RRBS).

2 | MATERIALS AND METHODS

2.1 | Animal model

As described previously,[6,7,24,25] time-of mating-matched, first-time pregnant, pair-fed, Sprague Dawley rat dams (F0) weighing 200–250 g received either placebo (saline, n = 3) or nicotine (1 mg/kg, subcutaneously, n = 4) in 100 μL volumes daily from embryonic day (e) 6 of gestation to postnatal day (PND) 21. The dose of nicotine used (1 mg/kg/day) is within the range of nicotine exposure in the moderately heavy smoker (5–9 cigarettes/day, 0.16 to 1.8 mg/kg body weight).[26–28] At this dose, the pulmonary structural, molecular, and functional changes that we observed in the rat model used are similar to those demonstrated in numerous other perinatal nicotine and smoke exposure models.[1,2,7,14,14,24,29]

Animals were maintained in a 12 hours: 12 hours light: dark cycle, pair-fed according to the previous day's food consumption by the nicotine-treated group, and were allowed free access to water. Following spontaneous delivery at term, the F1 pups were allowed to breastfeed ad libitum. At PND21, pups were weaned and maintained in separate cages. At PND60, males [n = 10 (from 3 to 4 separate litters) for each group] were euthanized by pentobarbital overdose injected intraperitoneally, followed by epididymis and lung collections as quickly as possible. The lungs were flash-frozen in liquid nitrogen and kept at −80°C for later qRT-PCR and Western blot analyses. The epididymides were kept in ice-cold F12 culture medium until sperm isolation within 1–2 hours of the collection, as outlined below. All animal procedures were performed following the National Institutes of Health

guidelines for the care and use of laboratory animals and approved by the Institutional Animal Care and Use Committee at The Lundquist Institute for Biomedical Innovation at Harbor-UCLA Medical Center.

2.2 | Isolation of sperm cells

At culling, each epididymis was isolated by cutting the vas deferens and muscle connections with the testis. After trimming the surrounding connective tissue, the two epididymides from each animal were placed in a tissue culture plate containing 3 mL of F12 culture medium on ice. The spermatozoa were released into the culture media by making 6–8 small cuts to each epididymis with a sharp blade, and the plates were placed in a culture incubator at 37°C for 30 minutes. Following incubation, the medium containing spermatozoa was filtered through a cell strainer (Genesee Scientific, 70 μm Advanced Cell Strainers, Cat No. 25–376) to a 50 mL conical tube, and the filtrate was divided into four 1.5 mL micro-centrifuge tubes. The tubes were centrifuged at 1000 *g* for 5 minutes, supernatants discarded, and 1 mL lysis buffer (0.05% SDS and 0.005% triton X-100 in distilled water) added to each tube to gently suspend the pellet. The tubes were kept on ice for 5 minutes to lyse and remove the contaminated somatic cells. After confirming the purity of isolated sperms microscopically, the samples were centrifuged at 3000 *g* for 5 minutes. The supernatants were discarded, and each pellet gently suspended in 1 mL ice-cold PBS. The suspensions from two tubes were pooled and centrifuged at 3000 *g* for 5 minutes. The supernatants were discarded, and pellets stored at −80°C until DNA isolation.

2.3 | Sperm DNA extraction

For isolation of total genomic DNA from epididymal spermatozoa, an aliquot of about 40 μL of the sperm pellet was used in a QIAamp DNA Mini Kit (Qiagen, Germany, Cat. No. 51304) according to the instructions of the manufacturer. The concentration and purity of the DNA were determined using a Thermo Scientific NanoDrop 2000 spectrophotometer.

2.4 | Library preparation of reduced representation bisulfite sequencing

RRBS libraries were prepared as previously described.[30–32] Briefly, genomic DNA was incubated with Msp1 (NEB, Frankfurt, Germany) restriction enzyme overnight for fragmentation. Adenylation step was performed using dNTP and Klenow fragment followed by an AMPure Bead clean-up (Beckman Coulter, Copenhagen, Denmark) and ligation to TruSeq adapters (Illumina, CA, USA). All the samples were pooled and subjected to bisulfite conversion using the EZ DNA Methylation Kit (Zymo Research, Freiburg, Germany). The library pool was amplified by PCR (2 min 95°C [30 s 95°C, 30 s 65°C; 45 s 72°C] × 20 cycles; 7 min 72°C) with PfuTurbo Hotstart DNA polymerase (Agilent, Glostrup, Denmark). PCR products were purified using the AMPure Bead clean-up. Libraries were sequenced on a NextSeq 500 system (Illumina), on a 75-bp single-end sequencing mode.

2.5 | RNA Isolation and quantitative polymerase chain reaction (qPCR) analysis

Total RNA from lung specimens was extracted using Trizol (Thermo Fisher Scientific, Waltham, MA). The quantity and quality of the isolated RNA was determined

by spectrophotometry (ND-1000, NanoDrop Technologies, Wilmington, DE, USA) as previously described.[33] RNA sample of 1 μg each was reverse transcribed using random primers. Quantitative RT-PCR was carried out using SYBR gene expression master mixes (Applied Biosystems, Carlsbad, CA). The PCR reaction was: 10 minutes 95°C followed by 40 cycles of 15 seconds at 95°C and 1 minutes at 60°C. Expression levels were quantified using the Invitrogen StepOne System and normalized to *ppia*. All reactions were run in triplicate and relative expression was determined using the comparative cycle threshold method ($2^{\Delta\Delta CT}$), as recommended by the supplier (Applied Biosystems). Abundance values were expressed as fold changes compared to the placebo treatment group. The primer sequences used in the study are listed in Table 1.

2.6 | Immunoblotting

The isolated lungs were flash-frozen in liquid nitrogen and then homogenized and sonicated in four volumes of ice-cold cell lysis buffer containing 50 mM β-glycerophosphate (pH 7.4), 150 mM NaCl, 1.5 mM EGTA, 1 mM EDTA, 1% Triton X-100, 100 mM NaF, 2 mM Na3VO4, 1 mM dithiothreitol, 1 mM phenylmethylsulfonyl fluoride, 1 mM benzamidine, 10 μg/mL leupeptin, 10 μg/mL aprotinin, and 2 μg/mL pepstatin A. After centrifugation at 13 200 *g* for 15 min at 4°C, the supernatant was used for Western blot analysis to determine protein levels of fibronectin, α smooth muscle actin (αSMA), calponin, collagen I & III, nicotinic acetylcholine receptor (nAChR) α3 and α7, β-catenin, lymphoid enhancer-binding factor-1 (LEF-1) and peroxisome proliferator-activated receptor gamma (PPARγ). The total protein concentration of the supernatant was measured using the Pierce BCA Protein Assay Kit (Thermo Scientific, USA, Cat. No.23225) with bovine serum albumin as the protein standard. Aliquots of the supernatant, each containing 30 μg of protein, were separated by SDS-PAGE and transferred to nitrocellulose membranes. Non-specific binding sites were blocked with Tris-buffered saline (TBS) containing 5% non-fat dry powdered milk (wt/vol) for 1 hour at room temperature. After a brief rinse with TBS containing 0.1% Tween 20 (TBST), the protein blots were incubated in 1:250 diluted anti-fibronectin monoclonal antibody (BD Biosciences, USA, Cat. No. 610078), 1:10 000 diluted anti-αSMA monoclonal antibody (Sigma-Aldrich, USA, Cat. No. A2547), 1:6000 diluted anti-calponin monoclonal antibody (Sigma-Aldrich, USA, Cat. No. C-2687), 1:500 diluted anti-collagen I polyclonal antibody (Fitzgerald Industries, USA, Cat. No. RDIMCOII1abr), 1:1000 diluted anti-collagen III monoclonal antibody (Sigma-Aldrich, USA, Cat. No. C7805), 1:400 diluted anti-nicotinic AChRα3 (Santa Cruz Biotechnology, USA, Cat. No. sc-5590), 1:20 000 diluted anti-nicotinic AChRα7 (Sigma-Aldrich, USA, Cat. No. N8158), 1:1000 diluted anti-β-catenin (Santa Cruz Biotechnology, USA, Cat. No. sc-7963), 1:500 diluted anti-LEF-1 (Santa Cruz Biotechnology, USA, Cat. No. sc-28687), 1:1000 diluted anti-PPARγ (Santa Cruz Biotechnology, USA, Cat. No. sc-7196), and 1:4000 diluted anti-GAPDH monoclonal antibody (MilliporeSigma, USA, Cat. No. MAB374,) overnight at 4°C. After washes with TBST, blots were incubated in 1:1000 (fibronectin), 1:10 000 (αSMA), 1:6000 (calponin), 1:2500 (collagen I), 1:2000 (collagen III), 1:3000 (AChRα3), 1:20 000 (AChRα7), 1:2500 (β-catenin, LEF-1, and PPARγ), and 1:4 000 (GAPDH) diluted horseradish peroxidase-conjugated anti-mouse, rat, or rabbit secondary antibody for 1 hour at room temperature. Blots were exposed to X-ray film using HyGLO Chemiluminescent Antibody Detection Reagent (Denville Scientific, USA, Cat. No. E-2500) and developed.

The relative densities of the protein bands were determined with ImageJ software and normalized to the density of GAPDH.

2.7 | Data analysis

2.7.1 | Statistical analysis of RRBS—RRBS reads in FASTQ format were trimmed using Trim Galore! v0.4.3 with the --rrbs flag. On average, 22.8 million trimmed reads per sample were aligned to rat genome (rn6, release 92, Ensembl),[34] and methylation levels estimated using Bismark[35] v0.18.1 using Bowtie 2[36] v2.2.5 on default settings. The SNPs from dbSNP database[37] (build 149, Rnor_6.0) and CpGs with coverage larger than 10 times the 95-percentile of coverage in each sample were filtered out. CpGs were aggregated within each gene and promoter (from 2000 bp upstream to 1000 bp downstream of TSS) regions. Differential methylation analysis was performed by edgeR[38] v3.24.0 for CpG sites (n = 171 768), genes (n = 10 948), and promoters (n = 7444). CpGs with a minimum of 10 counts were considered for differential methylation analysis and CpGs (in promoters or gene bodies) with an adjusted p-value (FDR) below 0.05 were considered as differentially methylated. The ratio of methylated CpGs to unmethylated CpGs (M-value) was used for multi-dimensional scaling (MDS) analysis.

The methylation percentages for genomic regions, gene bodies, promoters, 5′-UTRs, exons, introns and 3′-UTRs were calculated by aggregating the single CpG methylation levels from RRBS analysis. Since the assumptions of parametric testing were violated, a non-parametric test similar to 2-way ANOVA setup, Scheirer-Ray-Hare test, was performed considering methylation level as dependent parameter (m), while genomic region (g) and nicotine treatment (t) were considered as independent parameters (m ~ g + t). Dunn test was performed as a post-hoc test to identify pairwise comparisons. All sequencing data is stored in Gene Expression Omnibus (GEO) database with accession number GSE173898 (https://www.ncbi.nlm.nih.gov/geo/query/acc.cgi?acc=GSE173898).

2.8 | Pathway enrichment analysis

FRY algorithm, implemented in edgeR[38] R package, was used to identify enriched pathway terms from GO (BP, biological process) database.[39] Using an FDR cut-off of 0.05, 39 and 3 enriched terms were identified for genes and promoters, respectively. As there were many redundant terms in the enriched pathway terms, a clustering approach was applied to simplify the terms into relevant categories. First, the pathway terms were connected if two terms had at least one shared gene. The interaction network among the enriched terms was created by this criterion forming nodes as enriched terms and edges (vertices) as connection between the two terms. Linked-communities were identified by linkcomm[40] R package using “single” distance metric and “ward.D2”[41] algorithm resulting in 11 linked-communities. The different linked-communities can share the same GO term, which explains the biological relatedness of diverse linked-communities. We then used the linked-communities to find out the similar biological pathways clustered into smaller groups by using hierarchical clustering with “binary” distance and “ward.D2”[41] algorithm, which ended up forming 6 distinct clusters identified by dynamic TreeCut algorithm[42] with “hydrid” method and minimum cluster size of 3 GO terms.

2.9 | Statistical analysis of qPCR and Western blot data

The qPCR ΔCt values of each gene of interest (GOI) were normalized to fold-changes by comparing to housekeeping gene *Ppia*. The outliers were removed using Grubb's test.[43] As the assumption of normality was violated (Shapiro test, $P < .05$), a non-parametric, Wilcoxon Rank-Sum, test was done for each gene expression. The resulting p-values were adjusted for multiple testing by Benjamini Hochberg[44] method. The genes with FDR below 0.05 were considered differentially expressed. Western blots images were scanned, and background normalized by using ImageJ software (National Institutes of Health, Bethesda, MD., USA, https://imagej.nih.gov/ij/download.html). The relative signal intensity of the imaging data was analyzed using a similar statistical approach used for the RT-qPCR anlysis.

3 | RESULTS

3.1 | Nicotine treatment affects CpG methylation levels of F1 spermatozoa

Rat F0 females (E6 - PND21) were subcutaneously administered either nicotine (1 mg/kg once daily) or saline as placebo. Spermatozoa of F1 male offspring (postnatal day 60, n = 10, from 3–4 separate litters in each group) were collected and subjected to RRBS (Figure 1A). Multidimensional scaling analysis showed that nicotine and placebo treatment had a distinct separation across individual CpG profiles (Figure 1B). To identify if global methylation level in specific genomic region is changed by nicotine exposure, CpGs were aggregated into several genomic regions, including gene bodies, promoters, 5′-UTRs, exons, introns, and 3′-UTRs. While treatment with nicotine did not have an overall significant effect over placebo treatment (Scheirer–Ray–Hare Test, $p_{\text{treatment}} = 0.79$), specific genomic regions showed significant differences between each other (Scheirer–Ray–Hare Test, $p_{\text{region}} = 0$). Dunn post-hoc test for pairwise comparisons identified that almost all genomic regions had different methylations levels (Table 2). Introns exhibited the highest global CpG methylation levels, followed by gene bodies, 3′-UTRs, and exons. The smallest methylation levels were observed in 5′-UTRs and promoters (Figure 1C).

After filtering low count methylated CpGs and SNPs, 171 768 CpGs were considered for RRBS differential methylations analysis. CpGs with an FDR below 0.05 were considered differentially methylated (Table S1A). Mean percent methylation between nicotine and placebo groups had high correlation (Pearson correlation, $\rho = 0.994$), which indicates that the majority of the CpG methylation is not affected by the treatment (Figure 1D). In line with the observations shown in Figure 1B, hierarchical clustering of M-values, which is defined as the ratio between methylated and unmethylated CpG counts, showed that all sperm samples from nicotine and placebo groups were clustered separately (Figure 1E). We identified 39 hypomethylated and 42 hypermethylated CpGs ($n_{\text{total}} = 81$) as differentially methylated (Table S1A).

3.2 | Differentially methylated regions are more frequent in gene bodies than promoters

To identify the differentially regulated genes or promoters, the CpGs inside each genomic region were aggregated. CpG aggregation in these genomic regions resulted in 10 948 gene bodies and 7444 promoters. Differential methylation analysis identified 16 gene bodies and

3 promoters differentially methylated (Figure 2, Table S1B,C). Hierarchical clustering of percent methylation levels returned two separate clusters of nicotine and placebo treatment groups in both genes and promoters (Figure 2B,D). The only exception in differentially methylated promoters was rat #6 (denoted as Nico-6).

3.3 | Differential methylation of nicotine-response genes in spermatozoa

To identify the gene pathways which may be coordinately affected by CpG methylation upon nicotine exposure, we ran a gene enrichment analysis using FRY algorithm in edgeR R package.[38] We found 38 genes and 3 promoters enriched for Gene Ontology Biological Processes (GO, BP) (Table S2). The term "response to oxidative stress" was the only enriched term shared between genes and promoters. GO terms with shared genes with similar function were grouped into 11 different categories, called *linked-communities* (see Materials and Methods for details) (Figure 3A,B). To identify the groups of GO terms similar to each other, linked-communities were clustered using hierarchical clustering, which resulted in 6 different clusters (Figure 3C).

Of the GO clusters identified, Cluster 1 contains GO terms related to development and response to cellular stress like "lung alveolus development", "limb development", and "brain development" as well as "response to oxidative stress" and "platelet aggregation". Strikingly, nicotine treatment was associated to methylation of genes involved in "response to nicotine," while genes in this GO term were shared with other stress responses and developmental processes. Cluster 2 contains the GO terms involved in metabolic processes related to oxidative stress response, similar to cluster 1, such as "regulation of glutathione biosynthetic process", "regulation of cysteine metabolic process", "dipeptide import across plasma membrane" and "regulation of cellular response to oxidative stress". Cluster 3 contains GO terms enriched mainly for terms related to cellular signaling, DNA damage, and transcription. Of interest, the c-Jun N-terminal kinase (JNK) pathway, which is activated upon ionizing γ-radiation, UV, and nicotine[45,46] is a member of cluster 3. Similar to cluster 3, cluster 4 includes GO terms related to cellular signaling, but also terms related to transcriptional regulation. Cluster 5 GO terms are related to immune response, NF-κB transcriptional regulation by protein ubiqutination.[47,48] Lastly, genes in cluster 6 either do not overlap with the genes of other GO terms, thereby not a member of any linked-communities (eg "chloride transport"), or are unique to linked-communities. For example, "chromosome segregation" in cluster 6 is a member of linked-community #11, which is constituted of other cell cycle regulation terms including "negative regulation of transcription, DNA–templated" (cluster 4), "response to UV" and "cell cycle" (cluster 3) (Figure 3C).

3.4 | Differentially methylated regions in sperm may control gene expression in lung tissue

Previously, we reported in this cohort that perinatal nicotine treatment affects offspring lung development across generations.[6,49] Thus, since we identified "lung alveolus development" as one of the enriched GO terms upon nicotine treatment, we examined whether the methylation pattern of differentially methylated genes in sperm cell were associated with expression changes of the related genes in lung tissue. We investigated the top

10 differentially methylated genes, selected based on ranking highest absolute percent methylation difference with a lower FDR cut-off (FDR < 0.10) as a tradeoff between higher methylation difference and lower statistical significance. These DMRs had an average of more than 13% absolute methylation difference ($|\Delta\beta| > 0.13$) between control and treatment. Although the DMR next to the lncRNA AABR07046830.1 was in the top differentially methylated, it could not be reliably detected by qRT-PCR, possibly due to its short half-live (t1/2 RNA) (data not shown). Therefore, AABR07046830.1 was excluded from further gene expression analysis. We investigated the *Map4k2* since it shows the highest percent methylation (13.25%) of the differentially methylated promoters. In total, we investigated the expression pattern of 11 genes, which included AABR07051515.1, *Dio1*, *Gabra4*, *Htr6*, *Map4k2*, *Men1*, *Nmu*, *Orai2*, *Rars*, *Sec14l5*, and *Slc7a11* (Figure 4). Examining their expression profiles, AABR07051515.1 and *Dio1* were differentially expressed (FDR < 0.05) and *Map4k2* was near the threshold of significance (FDR =0.054). The highest hypermethylated ($\Delta\beta = 68.2\%$) gene was *Dio1*, which is iodothyronine deiodinase 1, and its gene expression was down-regulated 2.19-fold ($\log_2 FC = -1.13$) in the nicotine-treated group. The next highest hypermethylated gene was AABR07051515.1 ($\Delta\beta = 18.8\%$) and its transcript was up-regulated 1.55-fold ($\log_2 FC = 0.63$) (Figure 4).

3.5 | Key lung development and injury repair proteins had mixed gene expression patterns

Next, we measured the lung lysate levels of key lung development and injury repair proteins. The abundance of 10 key proteins involved in these processes and which are known to be affected by nicotine exposure[1,14,49–51]: AChRα3; AChRα7; αSMA; β-catenin; Calponin; Collagen I, Collagen III; Fibronectin; LEF1; and PPAR-γ (Figure 5 and Figure S1). While at the protein level, all of these gene products were significantly up-regulated upon nicotine exposure except PPAR-γ, at the transcript level, we did not detect a consistent pattern. Interestingly, AChRα7, β-catenin, and Calponin had up-regulated protein abundance while their gene expression levels were down-regulated. However, LEF1 and PPAR-γ congruent gene expression and protein abundance patterns, up-regulated and down-regulated, respectively (Figure 5).

4 | DISCUSSION

Our study shows that the epigenetic signature of spermatozoa of animals exposed to nicotine perinatally is altered. We identified striking DNA methylation changes at the proximity of genes controlling the response to nicotine and lung development. Given the transgenerational transmission of lung phenotype following perinatal nicotine exposure, the epigenetic alterations identified in spermatozoa may constitute a developmental reprogramming involved in the etiology of altered lung function later in life and transgenerationally.

In the same animal model and study design, we have previously reported that DNA methylation of the whole testicular tissue is increased at the global level in nicotine-exposed F1 offspring.[6,23] Here, we show that perinatal nicotine exposure did not change global DNA methylation in spermatozoa from F1 animals. This discrepancy may be due to DNA

methylation changes in a non-germ cell(s) in the testis or may be due to the difference in the assays performed between the studies. The global 5mC methylation profile was assessed by ELISA previously,[6,23] while here, we used the aggregate of individual CpG methylations to calculate the global DNA methylation by RRBS. RRBS is known to have a selection bias toward CpG islands since *MspI* digestion sites (CCGG) are enriched, which neglects 5mC sites elsewhere.[52] Similar to our findings using rat RRBS, Jenkins et. al. have shown that there are no significant differences between control and smoker sperm DNA methylation on gene bodies using Infinium HumanMethylation450 BeadChip microarrays (Illumina).[53]

Enrichment analysis of biological processes regulated by differentially methylated loci upon nicotine exposure identified six linked-community clusters. Interestingly, in line with the known effects of nicotine on the developing offspring,[1,14] we determined that genes involved in pathways controlling nicotine response, alveolar and brain development, cellular signaling, and oxidative stress were epigenetically remodeled. Of interest, the only GO term enriched in both differentially methylated promoters and gene body was “response to oxidative stress”. As DNA demethylation is dependent on oxidation processes,[17] and since nicotine treatment induces oxidative stress,[54,55] epigenetic reprogramming after perinatal nicotine exposure may be controlled, at least in part, by the oxidative stress caused by nicotine exposure.

To determine the potential developmental impact of nicotine-induced differential methylation changes in sperm cells of the perinatal nicotine-exposed offspring, we investigated the lung expression patterns of the genes located near the top 10 DMRs that we identified. Of these, only AABR07051515.1 and *Dio1* were differentially expressed, with varying effects of methylation status on gene expression. For example, the expression of the highest differentially hypermethylated gene *Dio1* in sperm cells was down-regulated in the nicotine-exposed group lungs, whereas the expression of AABR07051515.1, the next highest hypermethylated gene in sperm cells, was up-regulated in the lung. In contrast to the methylation of *a promoter*, which is classically associated with gene repression,[56] our results are consistent with previous observations that gene body methylation can affect gene expression both positively and negatively.[57] It is worth pointing that in a rat model of volutrauma-induced lung injury, which shares molecular similarities to nicotine-induced lung injury,[14] AABR07051515.1, a lincRNA, was down-regulated.[58] Thus, the AABR07051515.1 lincRNA may represent a target gene epigenetically remodeled by nicotine exposure, which plays a role in altered lung function in adult life.

Since perinatal nicotine exposure of F1 animals alters the lung phenotype of not only the F1 generation, but also the F2 and F3 generations,[6,7] epigenetic reprogramming of spermatozoa may represent a mechanism by which lung development is reprogrammed transgenerationally following perinatal nicotine exposure. Central to the mechanistic understanding of the transmission of any acquired phenotype across generations is understanding the difference between intergenerational and transgenerational transmission.[59,60] While intergenerational transmission implies the transmission of the effects of direct exposure of a non-mutagenic stimulus on the parental germline to children (F0 to F1 in our experimental setup), transgenerational transmission occurs when the affected offspring is not directly exposed to the non-mutagenic stimulus (F1 to F2/F3). Our

experimental setup does not allow to determine the causality between epigenetic changes in spermatozoa and the lung phenotype seen in the adult life and in future generations. Determination of sperm DNA profiles of F2 and F3 generation male offspring of F1 animals exposed to nicotine in utero may give further insight into the role of sperm DNA methylation on lung phenotype.

While in this study we focused on lung tissue, other tissues may also be affected by the spermatozoa's epigenetic reprogramming. Nicotine-induced transgenerational inheritance of other phenotypic and molecular traits has been described in other models.[61,62] Previous studies of paternal preconceptional exposure to nicotine showed higher tolerance to cocaine in the next generation.[63] Given the importance of the nicotinic pathway in brain function, notably in the reward system and substance addiction, the DNA methylation changes that we identified at the proximity of genes controlling the nicotine response may affect the expression of the related genes in the brain as well. Further investigations should be conducted to explore the possible link between reprogrammed epigenetic signature by perinatal exposure to nicotine and the characteristics of the nicotinic pathway in the brain of the adult.

Although there is a general agreement that gametic epigenetic marks are largely erased after fertilization,[22] there are unequivocal examples of retention of environmentally induced epigenetic marks across generations.[64–66] Since two rounds of nearly complete DNA demethylation occur during development, at the embryogenesis and at the gametogenesis stages, retention of environmentally changed DNA methylation is likely to be modest. Epigenetic signals other than DNA methylation might be at play in the transmission of transgenerational inheritance induced by nicotine exposure, for example, histone modifications and expression of small and long noncoding RNAs, as suggested in other models of epigenetic inheritance.[22] While other epigenetic marks than DNA methylation may be involved, our discovery that DNA methylation near genes involved in nicotine metabolism is altered in spermatozoa from animals exposed to nicotine strongly suggests that DNA methylation is involved in the inheritance of perinatal nicotine exposure. Whether the DNA methylation marks that we detected in sperm from exposed animals are directly responsible for the transmission of a phenotype in every generations affected downstream the nicotine-exposed animals (ie, in a true transgenerational fashion), or are leading to an altered phenotype in the next generation which reprograms the following generation in a serial manner cannot be determined at this stage.

In conclusion, our discovery that perinatal nicotine exposure remodels the spermatozoal epigenome of genes that control the response to nicotine strongly supports a functional role on the phenotype of the next generations. Strategies aiming to prevent or revert the reprogramming of the spermatozoa epigenome may constitute promising approaches to mitigate some of the effects of perinatal nicotine exposure on the developmental reprogramming of the next generation.

Supplementary Material

Refer to Web version on PubMed Central for supplementary material.

ACKNOWLEDGMENTS

We acknowledge the Single-Cell Omics platform at the Centre for Basic Metabolic Research (CBMR) for the technical expertise and support. This research received support from the NIH (HD071731, HD127237, HL151769, and HL152915) and the TRDRP (23RT-0018, 27IP-0050, and T29IR0737). This work was partly supported by a Challenge Programme Grant from the Novo Nordisk Foundation (NNF18OC0033754) to the Gametic Epigenetics Consortium against Obesity (GECKO). OF was recipient of a research grant from the Danish Diabetes Academy supported by the Novo Nordisk Foundation. The Novo Nordisk Foundation Center for Basic Metabolic Research is an independent research center at the University of Copenhagen, partially funded by an unrestricted donation from the Novo Nordisk Foundation (NNF18CC0034900).

Funding information

HHS | National Institutes of Health (NIH), Grant/Award Number: HD071731; HHS | National Institutes of Health (NIH), Grant/Award Number: HD127237; HHS | National Institutes of Health (NIH), Grant/Award Number: HL151769; HHS | National Institutes of Health (NIH), Grant/Award Number: HL152915; Tobacco-Related Disease Research Program (TRDRP), Grant/Award Number: 23RT-0018; Tobacco-Related Disease Research Program (TRDRP), Grant/Award Number: 27IP-0050; T-obacco-Related Disease Research Program (TRDRP), Grant/Award Number: T29IR0737; Novo Nordisk Fonden (NNF), Grant/Award Number: NNF18CC0034900; Novo Nordisk Fonden (NNF), Grant/Award Number: NNF18OC0033754

DATA AVAILABILITY STATEMENT

All sequencing data will available under Gene Expression Omnibus data repository.

Abbreviations:

DMR	differentially methylated region
DNMT	DNA methyltransferase
EDTA	ethylenediaminetetraacetic acid
EGTA	ethylene glycol-bis(β-aminoethyl ether)-N,N,N′,N′-tetraacetic acid
FDR	false discovery rate
GO	gene ontology
GOI	gene of interest
LEF-1	lymphoid enhancer-binding factor-1
MDS	multi-dimensional scaling
Na3VO4	sodium orthovanadate
nAChR	nicotinic acetylcholine receptor
PND	postnatal day
PPARγ	peroxisome proliferator-activated receptor gamma
RRBS	reduced representation bisulfite sequencing
SNP	Single nucleotide polymorphism
TET	ten-eleven translocation

αSMA	alpha smooth muscle actin

REFERENCES

1. Kuniyoshi KM, Rehan VK. The impact of perinatal nicotine exposure on fetal lung development and subsequent respiratory morbidity. Birth Defects Res. 2019;111:1270–1283. [PubMed: 31580538]
2. Maritz GS, Harding R. Life-long programming implications of exposure to tobacco smoking and nicotine before and soon after birth: evidence for altered lung development. Int J Environ Res Public Health. 2011;8:875–898. [PubMed: 21556184]
3. McEvoy CT, Spindel ER. Pulmonary effects of maternal smoking on the fetus and child: effects on lung development, respiratory morbidities, and life long lung health. Paediatr Respir Rev. 2017;21:27–33. [PubMed: 27639458]
4. Tager IB, Segal MR, Speizer FE, Weiss ST. The natural history of forced expiratory volumes. Effect of cigarette smoking and respiratory symptoms. Am Rev Respir Dis. 1988;138:837–849. [PubMed: 3202458]
5. Upton MN, Smith GD, McConnachie A, Hart CL, Watt GCM. Maternal and personal cigarette smoking synergize to increase airflow limitation in adults. Am J Respir Crit Care Med. 2004;169:479–487. [PubMed: 14630616]
6. Rehan VK, Liu J, Naeem E, et al. Perinatal nicotine exposure induces asthma in second generation offspring. BMC Med. 2012;10:129. [PubMed: 23106849]
7. Rehan VK, Liu J, Sakurai R, Torday JS. Perinatal nicotine-induced transgenerational asthma. Am J Physiol Lung Cell Mol Physiol. 2013;305:L501–L507. [PubMed: 23911437]
8. Baeza-Loya S, Viswanath H, Carter A, et al. Perceptions about e-cigarette safety may lead to e-smoking during pregnancy. Bull Menninger Clin. 2014;78:243–252. [PubMed: 25247743]
9. Kurti AN, Redner R, Lopez AA, et al. Tobacco and nicotine delivery product use in a national sample of pregnant women. Prev Med. 2017;104:50–56. [PubMed: 28789981]
10. Obisesan OH, Osei AD, Uddin SMI, et al. E-cigarette use patterns and high-risk behaviors in pregnancy: behavioral risk factor surveillance system, 2016–2018. Am J Prev Med. 2020;59: 187–195. [PubMed: 32362509]
11. Oncken C, Ricci KA, Kuo C-L, Dornelas E, Kranzler HR, Sankey HZ. Correlates of electronic cigarettes use before and during pregnancy. Nicotine Tob. 2017;19:585–590.
12. Hammer B, Wagner C, Divac Rankov A, et al. In utero exposure to cigarette smoke and effects across generations: a conference of animals on asthma. Clin Exp Allergy. 2018;48:1378–1390. [PubMed: 30244507]
13. Pierce RA, Nguyen NM. Prenatal nicotine exposure and abnormal lung function. Am J Respir Cell Mol Biol. 2002;26:10–13. [PubMed: 11751198]
14. Rehan VK, Asotra K, Torday JS. The effects of smoking on the developing lung: insights from a biologic model for lung development, homeostasis, and repair. Lung. 2009;187:281–289. [PubMed: 19641967]
15. Colombo G, Clerici M, Giustarini D, et al. Pathophysiology of tobacco smoke exposure: recent insights from comparative and redox proteomics. Mass Spectrom Rev. 2014;33:183–218. [PubMed: 24272816]
16. Spindel ER, McEvoy CT. The role of nicotine in the effects of maternal smoking during pregnancy on lung development and childhood respiratory disease. implications for dangers of E-cigarettes. Am J Respir Crit Care Med. 2016;193:486–494. [PubMed: 26756937]
17. Wu X, Zhang Y. TET-mediated active DNA demethylation: mechanism, function and beyond. Nat Rev Genet. 2017;18:517–534. [PubMed: 28555658]
18. Joubert BR, Felix JF, Yousefi P, et al. DNA methylation in newborns and maternal smoking in pregnancy: genome-wide consortium meta-analysis. Am J Hum Genet. 2016;98:680–696. [PubMed: 27040690]
19. Knopik VS, Maccani MA, Francazio S, McGeary JE. The epigenetics of maternal cigarette smoking during pregnancy and effects on child development. Dev Psychopathol. 2012;24:1377–1390. [PubMed: 23062304]

20. Suter MA, Anders AM, Aagaard KM. Maternal smoking as a model for environmental epigenetic changes affecting birthweight and fetal programming. Mol Hum Reprod. 2013;19:1–6. [PubMed: 23139402]
21. Lambers DS, Clark KE. The maternal and fetal physiologic effects of nicotine. Semin Perinatol. 1996;20:115–126. [PubMed: 8857697]
22. Daxinger L, Whitelaw E. Understanding transgenerational epigenetic inheritance via the gametes in mammals. Nat Rev Genet. 2012;13:153–162. [PubMed: 22290458]
23. Liu J, Yu C, Doherty TM, Akbari O, Allard P, Rehan VK. Perinatal nicotine exposure-induced transgenerational asthma: Effects of reexposure in F1 gestation. FASEB J. 2020;34(9):11444–11459. [PubMed: 32654256]
24. Liu J, Naeem E, Tian J, et al. Sex-specific perinatal nicotine-induced asthma in rat offspring. Am J Respir Cell Mol Biol. 2013;48:53–62. [PubMed: 23002101]
25. Liu J, Sakurai R, Rehan VK. PPAR-γ agonist rosiglitazone reverses perinatal nicotine exposure-induced asthma in rat offspring. Am J Physiol Lung Cell Mol Physiol. 2015;308:L788–L796. [PubMed: 25659902]
26. Erickson AC, Arbour LT. Heavy smoking during pregnancy as a marker for other risk factors of adverse birth outcomes: a population-based study in British Columbia, Canada. BMC Public Health. 2012;12:102. [PubMed: 22304990]
27. Maritz GS, Woolward K. Effect of maternal nicotine exposure on neonatal lung elastic tissue and possible consequences. South Afr Med J. 1992;81:517–519.
28. Matta SG, Balfour DJ, Benowitz NL, et al. Guidelines on nicotine dose selection for in vivo research. Psychopharmacology. 2007;190:269–319. [PubMed: 16896961]
29. Collins MH, Moessinger AC, Kleinerman J, et al. Fetal lung hypoplasia associated with maternal smoking: a morphometric analysis. Pediatr Res. 1985;19:408–412. [PubMed: 4000765]
30. Fabre O, Ingerslev LR, Garde C, Donkin I, Simar D, Barrès R. Exercise training alters the genomic response to acute exercise in human adipose tissue. Epigenomics. 2018;10:1033–1050. [PubMed: 29671347]
31. Andersen E, Ingerslev LR, Fabre O, et al. Preadipocytes from obese humans with type 2 diabetes are epigenetically reprogrammed at genes controlling adipose tissue function. Int J Obes. 2019;43:306–318.
32. Andersen E, Altintaş A, Andersson-Hall U, Holmäng A, Barrès R. Environmental factors influence the epigenetic signature of newborns from mothers with gestational diabetes. Epigenomics. 2019;11:861–873. [PubMed: 30966798]
33. Chuang T-D, Ansari A, Yu C, et al. Mechanism underlying increased cardiac extracellular matrix deposition in perinatal nicotine-exposed offspring. Am J Physiol Heart Circ Physiol. 2020;319:H651–H660. [PubMed: 32795172]
34. Cunningham F, Achuthan P, Akanni W, et al. Ensembl 2019. Nucleic Acids Res. 2019;47:D745–D751. [PubMed: 30407521]
35. Krueger F, Andrews SR. Bismark: a flexible aligner and methylation caller for Bisulfite-Seq applications. Bioinformatics. 2011;27:1571–1572. [PubMed: 21493656]
36. Langmead B, Salzberg SL. Fast gapped-read alignment with Bowtie 2. Nat Methods. 2012;9:357–359. [PubMed: 22388286]
37. Sherry ST. dbSNP: the NCBI database of genetic variation. Nucleic Acids Res. 2001;29:308–311. [PubMed: 11125122]
38. Robinson MD, McCarthy DJ, Smyth GK. edgeR: a Bioconductor package for differential expression analysis of digital gene expression data. Bioinformatics. 2010;26:139–140. [PubMed: 19910308]
39. Gene Ontology Consortium. The Gene Ontology (GO) database and informatics resource. Nucleic Acids Res. 2004;32(90001):D258–D261. [PubMed: 14681407]
40. Kalinka AT, Tomancak P. linkcomm: an R package for the generation, visualization, and analysis of link communities in networks of arbitrary size and type. Bioinformatics. 2011;27:2011–2012. [PubMed: 21596792]
41. Murtagh F, Legendre P. Ward's hierarchical agglomerative clustering method: which algorithms implement ward's criterion? J Classif. 2014;31:274–295.

42. Langfelder P, Zhang B, Horvath S. Defining clusters from a hierarchical cluster tree: the Dynamic Tree Cut package for R. Bioinformatics. 2008;24:719–720. [PubMed: 18024473]
43. Grubbs FE. Sample criteria for testing outlying observations. Ann Math Stat. 1950;21:27–58.
44. Benjamini Y, Hochberg Y. Controlling the false discovery rate: a practical and powerful approach to multiple testing. J R Stat Soc Ser B Methodol. 1995;57:289–300.
45. Xue MQ, Liu XX, Zhang YL, Gao FG. Nicotine exerts neuroprotective effects against β-amyloid-induced neurotoxicity in SH-SY5Y cells through the Erk1/2-p38-JNK-dependent signaling pathway. Int J Mol Med. 2014;33:925–933. [PubMed: 24481039]
46. Li Z-Z, Guo Z-Z, Zhang Z, et al. Nicotine-induced upregulation of VCAM-1, MMP-2, and MMP-9 through the α7-nAChR-JNK pathway in RAW264.7 and MOVAS cells. Mol Cell Biochem. 2015;399:49–58. [PubMed: 25381636]
47. Chen ZJ. Ubiquitin signaling in the NF-κB pathway. Nat Cell Biol. 2005;7:758–765. [PubMed: 16056267]
48. Chen J, Chen ZJ. Regulation of NF-κB by ubiquitination. Curr Opin Immunol. 2013;25:4–12. [PubMed: 23312890]
49. Rehan VK, Wang Y, Sugano S, et al. In utero nicotine exposure alters fetal rat lung alveolar type II cell proliferation, differentiation, and metabolism. Am J Physiol Lung Cell Mol Physiol. 2007;292:L323–L333. [PubMed: 17215434]
50. Gong M, Liu J, Sakurai R, Corre A, Anthony S, Rehan VK. Perinatal nicotine exposure suppresses PPARγ epigenetically in lung alveolar interstitial fibroblasts. Mol Genet Metab. 2015;114: 604–612. [PubMed: 25661292]
51. Sakurai R, Cerny LM, Torday JS, Rehan VK. Mechanism for nicotine-induced up-regulation of Wnt signaling in human alveolar interstitial fibroblasts. Exp Lung Res. 2011;37:144–154. [PubMed: 21133803]
52. Sun Z, Cunningham J, Slager S, Kocher J-P. Base resolution methylome profiling: considerations in platform selection, data preprocessing and analysis. Epigenomics. 2015;7:813–828. [PubMed: 26366945]
53. Jenkins TG, James ER, Alonso DF, et al. Cigarette smoking significantly alters sperm DNA methylation patterns. Andrology. 2017;5:1089–1099. [PubMed: 28950428]
54. Guan Z-Z, Yu W-F, Nordberg A. Dual effects of nicotine on oxidative stress and neuroprotection in PC12 cells. Neurochem Int. 2003;43:243–249. [PubMed: 12689604]
55. Yildiz D, Ercal N, Armstrong DW. Nicotine enantiomers and oxidative stress. Toxicology. 1998;130:155–165. [PubMed: 9865482]
56. Newell-Price J, Clark AJ, King P. DNA methylation and silencing of gene expression. Trends Endocrinol Metab. 2000;11: 142–148. [PubMed: 10754536]
57. Yang X, Han H, De Carvalho DD, Lay FD, Jones PA, Liang G. Gene body methylation can alter gene expression and is a therapeutic target in cancer. Cancer Cell. 2014;26:577–590. [PubMed: 25263941]
58. Nonas SA, Moreno-Vinasco L, Ma SF, et al. Use of consomic rats for genomic insights into ventilator-associated lung injury. Am J Physiol Lung Cell Mol Physiol. 2007;293:L292–302. [PubMed: 17468131]
59. Cavalli G, Heard E. Advances in epigenetics link genetics to the environment and disease. Nature. 2019;571:489–499. [PubMed: 31341302]
60. Hanson MA, Skinner MK. Developmental origins of epigenetic transgenerational inheritance. Environ Epigenetics. 2016;2:dvw002.
61. McCarthy DM, Morgan TJ, Lowe SE, et al. Nicotine exposure of male mice produces behavioral impairment in multiple generations of descendants. PLoS Biol. 2018;16:e2006497. [PubMed: 30325916]
62. Taki FA, Pan X, Lee M-H, Zhang B. Nicotine exposure and transgenerational impact: a prospective study on small regulatory microRNAs. Sci Rep. 2014;4:7513. [PubMed: 25515333]
63. Vallaster MP, Kukreja S, Bing XY, et al. Paternal nicotine exposure alters hepatic xenobiotic metabolism in offspring. eLife. 2017;6:e24771. [PubMed: 28196335]

64. Dias BG, Ressler KJ. Parental olfactory experience influences behavior and neural structure in subsequent generations. Nat Neurosci. 2014;17:89–96. [PubMed: 24292232]

65. Morgan HD, Sutherland HG, Martin DI, Whitelaw E. Epigenetic inheritance at the agouti locus in the mouse. Nat Genet. 1999;23:314–318. [PubMed: 10545949]

66. Seong K-H, Li D, Shimizu H, Nakamura R, Ishii S. Inheritance of stress-induced, ATF-2-dependent epigenetic change. Cell. 2011;145:1049–1061. [PubMed: 21703449]

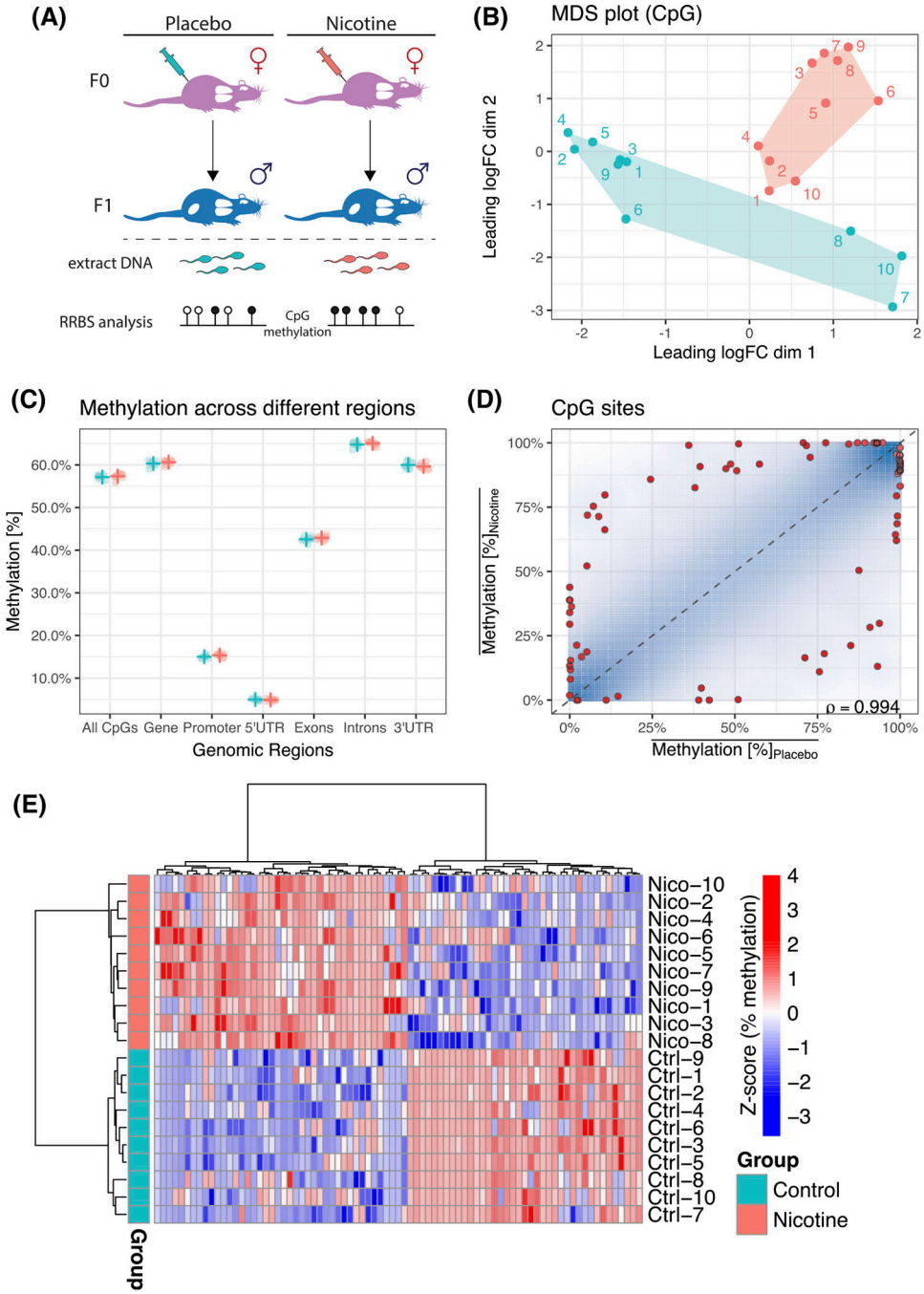

FIGURE 1.

A, Experimental setup. Rat F0 mothers (E6 - PND21) were injected with nicotine subcutaneously (1 mg/kg/od) or with saline as placebo. Sperm cells of male rats (PND60) were collected and DNA was extracted from sperm samples. Afterwards, the reduced representation bisulfite sequencing (RRBS) was performed. B, Multi-dimensional scaling (MDS) plot of leading logFC dimension 1 and 2 of DNA methylation data from individual CpG sites. The CpG profiles of placebo and nicotine-treated sperm cells were clustered in different groups. Green: placebo, red: nicotine-treated. C, Methylation percentage across

different genomic regions as all CpGs (global DNA methylation), gene bodies, promoters, 5′-UTRs, exons, introns and 3′-UTRs. The nicotine treatment did not affect the overall methylation between the two groups ($P = .79$, Scheirer–Ray–Hare Test), while individual genomic regions had significantly different methylation percentages ($P = 0$, Scheirer–Ray–Hare Test). X-axis: genomic regions, y-axis: Methylation percentage. Pairwise post-hoc comparisons (Dunn Test) for the genomics regions can be found on Table 2. Green: placebo, red: nicotine-treated. Solid horizontal lines show mean and solid vertical lines represent standard deviation. D, Comparison of the percent methylation of CpGs in placebo and nicotine-treated sperm samples. Red dots represent significant (FDR < 0.05) differentially methylated regions (DMRs). Faded blue shows the smoothed density for CpG sites and CpGs with no significant change upon nicotine treatment are expected to be on the diagonal line (dashed blue). E, Heatmap of differentially methylated individual CpG sites (FDR < 0.05). Heatmap colors indicate percent methylation values (z-score transformed; red, high; blue, low). Hierarchical clusters are calculated by ‘ward.D2’ algorithm using Pearson distance. Group colors; green, placebo; red, nicotine-treated

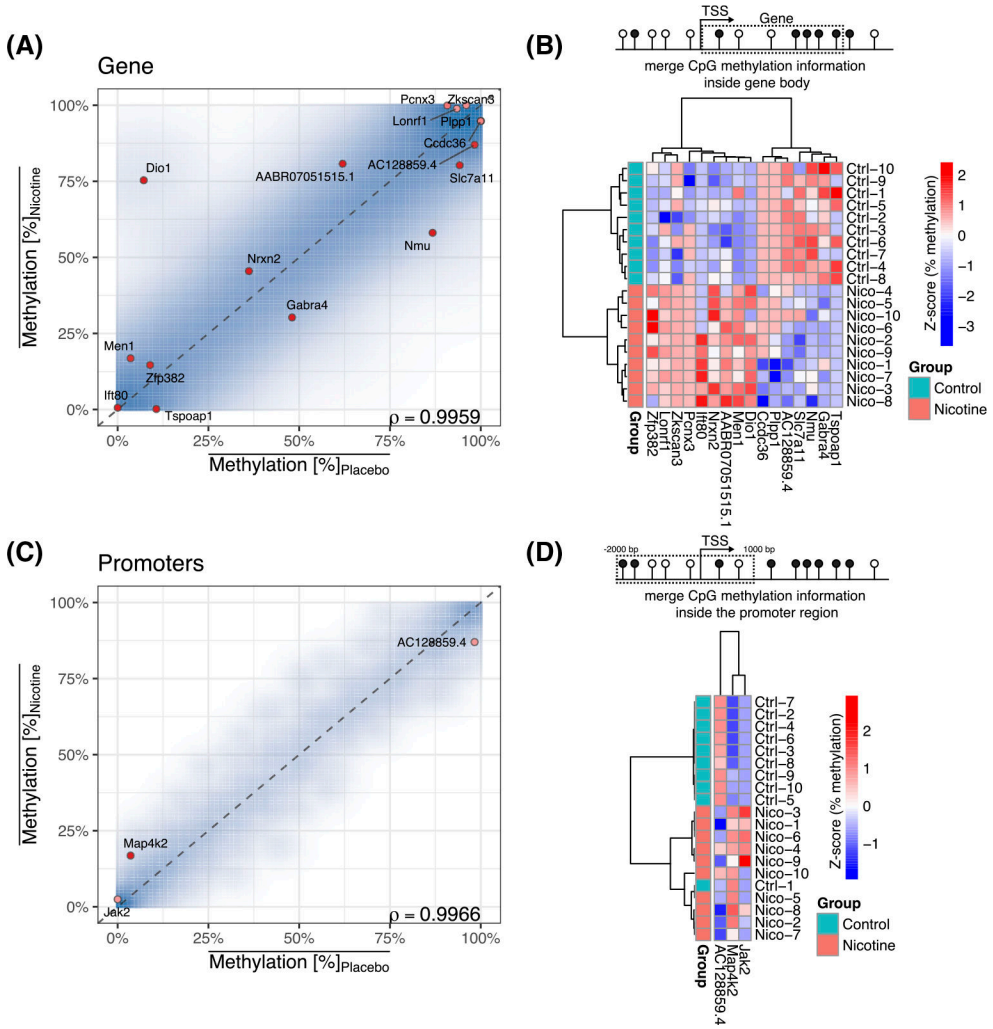

FIGURE 2.

Comparison of the percentage methylation of gene bodies (A) and promoters (C) in placebo and nicotine-treated sperm samples. Red dots represent significant (FDR < 0.05) differentially methylated regions (DMRs). Faded blue show the smoothed density for CpG sites. Heatmap of differentially methylated gene bodies (B) and promoters (D) (FDR < 0.05). Heatmap colors indicate percent methylation values (z-score transformed; red, high; blue, low). Hierarchical clusters are calculated by ‘ward.D2’ algorithm using Pearson distance. Group colors; green, placebo; red, nicotine-treated. Individual CpG sites are aggregated into gene bodies as the region from transcription start site (TSS) until 5′-UTR and promoters as the region from −2000 bp to +1000 bp from TSS

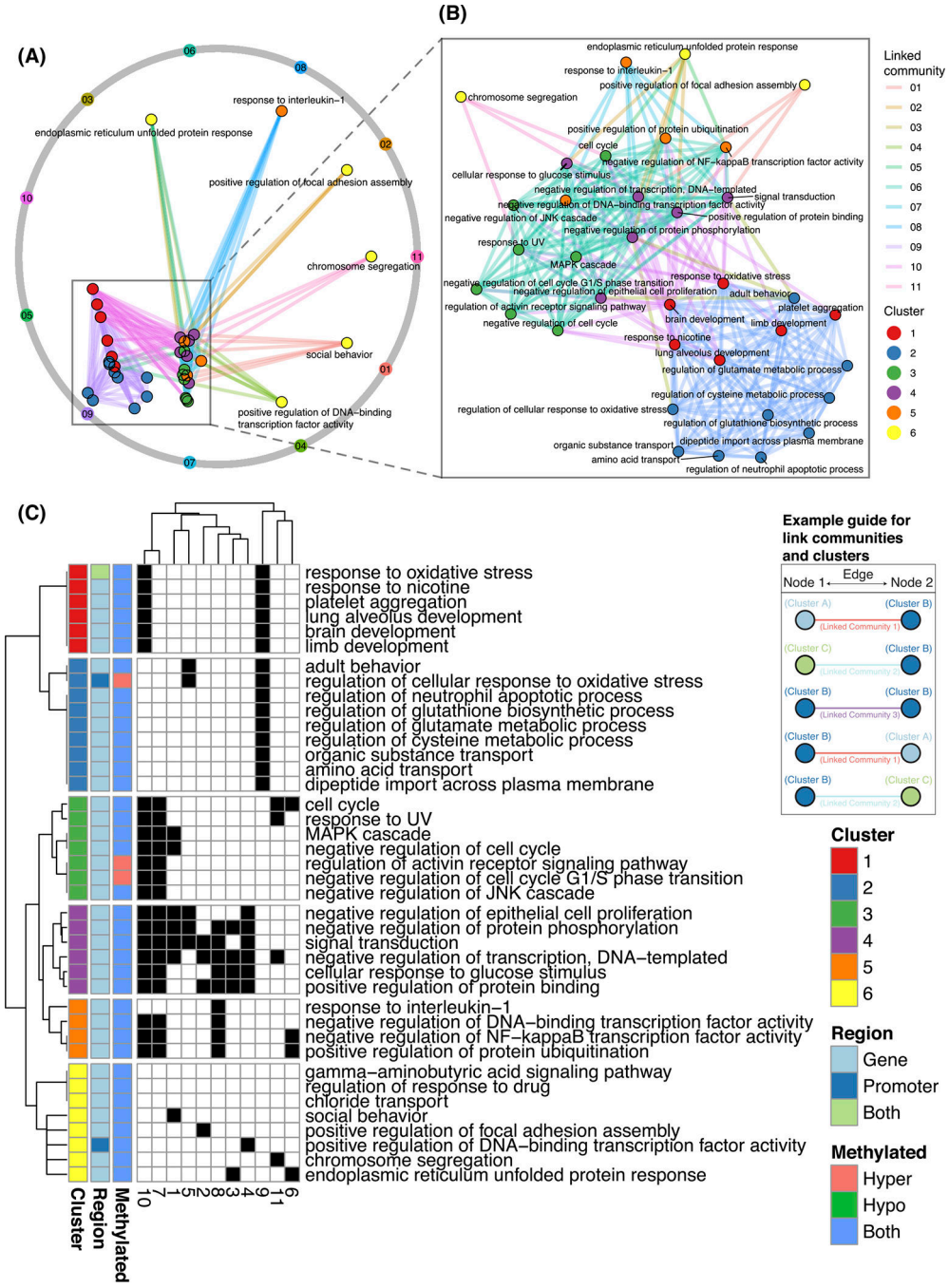

FIGURE 3.

Pathway enrichment analysis from CpG methylation (RRBS) results. Pathway enrichment was performed using FRY algorithm with GO database (Biological Process, BP, domain). A, All enriched pathways were connected to each other using the shared gene information. Linked-communities (n = 11) identifying the shared properties across all enriched pathways were calculated. The names show uniquely enriched terms. B, Enriched pathway terms were shared by multiple linked-communities. The view is zoomed in from the region defined by the rectangle in panel A. C, Hierarchical clustering of all pathway linked-communities

resulted in 6 unique clusters. Cluster 1: nicotine response, alveolar and brain development; Cluster 2: oxidative stress response; Cluster 3: cellular signaling and cell cycle; Cluster 4: cellular signaling and transcriptional regulation; Cluster 5: NF-κB transcriptional regulation by protein ubiquitination; Cluster 6: GO terms with no shared genes between each other, and GO terms unique to specific linked-communities

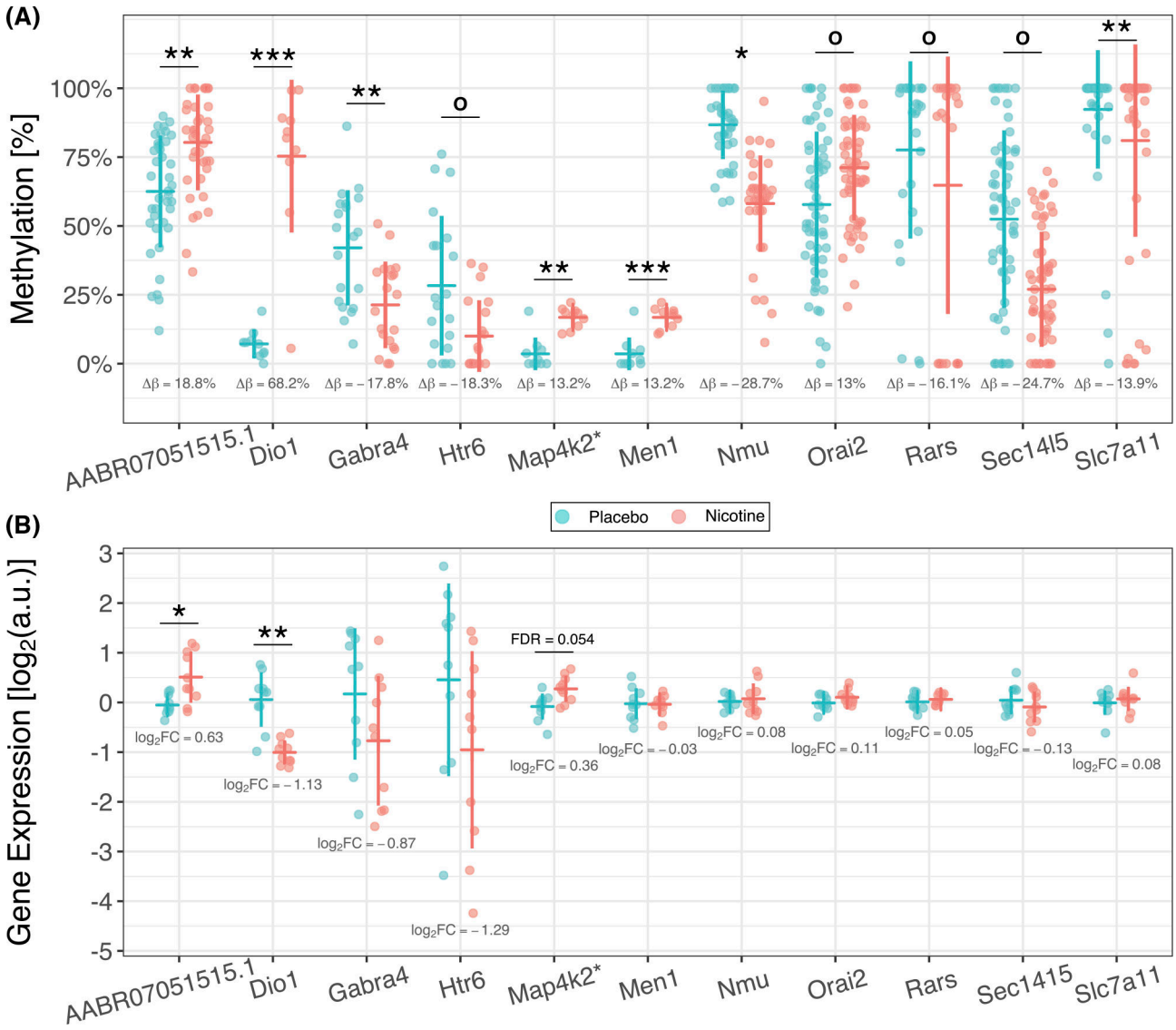

FIGURE 4.

A, Top selected differentially methylated genes for further downstream investigation. Each panel represents a gene except Map4k2, denoted with *, which is a differentially methylated promoter. x-axis: Genes presented with placebo or nicotine treatment groups; y-axis: methylation percentage; each dot represents a CpG site. The mean methylation difference between nicotine and placebo treatment is shown at the bottom of each panel. B, qPCR comparisons of top selected differentially methylated genes from lung. x-axis: treatment with placebo or nicotine; y-axis: Relative expression values of each gene of interest (GOI) compared to housekeeping gene PPIA; each dot represents a replicate (n = 10). Solid horizontal lines show mean and solid vertical lines represent standard deviation. The log2-fold change (log_2FC) between nicotine and placebo treatment is shown at the bottom of each panel. Genes with an FDR cutoff of 0.05 (Wilcoxon test) were considered to be differentially expressed. Significance stars are defined with the following acronyms: ***FDR < 0.001; **FDR < 0.01; *FDR < 0.05; ° FDR < 0.1

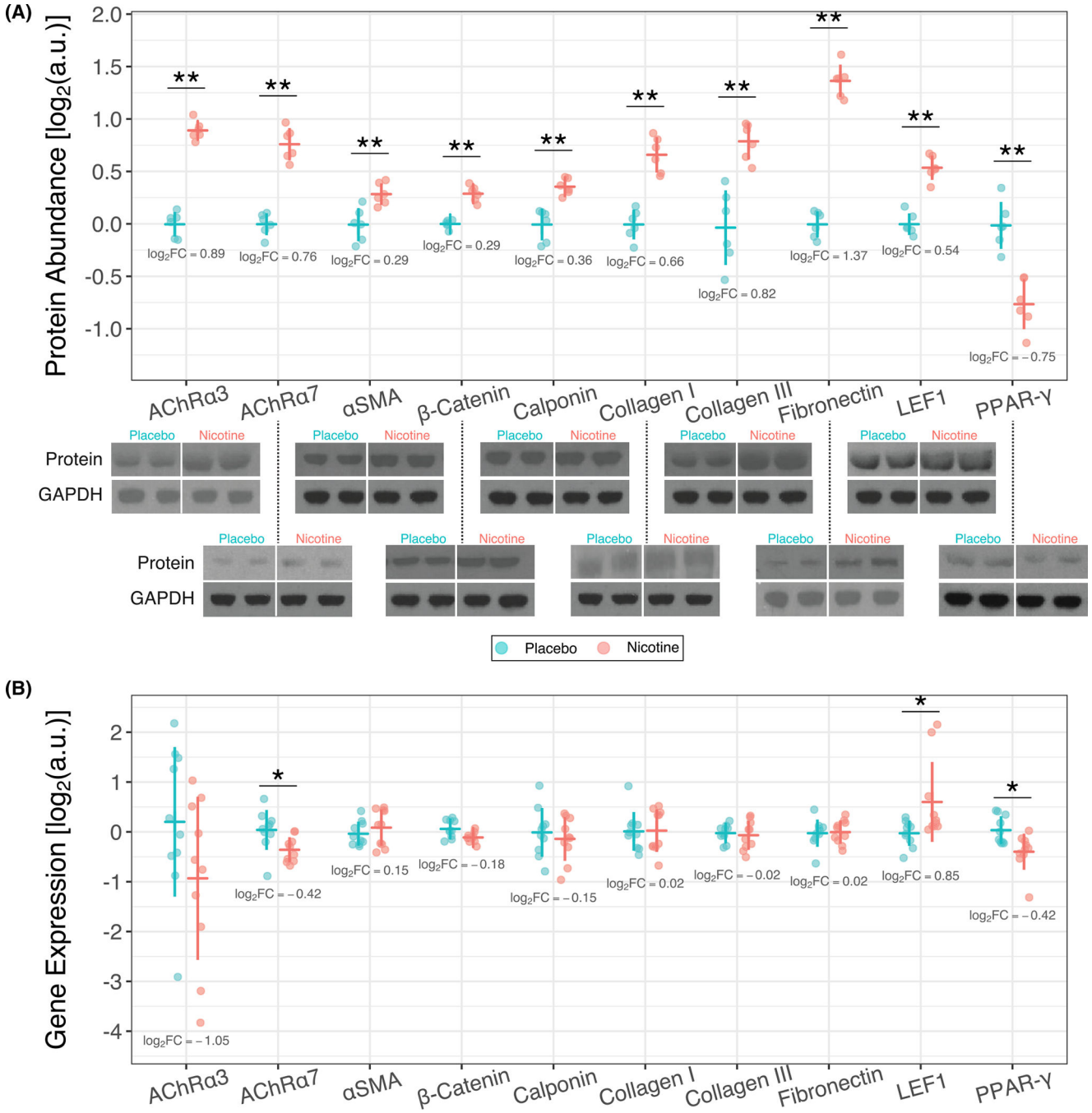

FIGURE 5.

A, Western blot (WB) analysis of key lung development and injury repair proteins in lung. x-axis: Proteins presented with placebo or nicotine treatment groups; y-axis: relative log2 intensity; each dot represents a replicate (n = 6). The mean protein level difference between nicotine and placebo treatment are shown at the bottom of each panel. A representative WB gel image for the given protein is shown under each panel. B (all original protein and GAPDH bands are shown in Figure S1), qPCR comparisons of genes shown in panel A from lung. x-axis: Genes presented with placebo or nicotine treatment groups; y-axis: Relative

expression values of each gene of interest (GOI) compared to housekeeping gene ppia; each dot represents a replicate (n = 10). Solid horizontal lines show mean and solid vertical lines represent standard deviation. The log2-fold change (log_2FC) between nicotine and placebo treatment is shown at the bottom of each panel. Proteins/genes with an FDR cutoff of 0.05 (Wilcoxon test) were considered to be differentially regulated. Significance stars are defined with following acronyms: ***FDR < 0.001; **FDR < 0.01; *FDR < 0.05; °FDR < 0.1

TABLE 1

Primer sequences used for qRT-PCR

Primers	Sequences
PPIA (Forward)	5′-GGCTATAAGGGTTCCTCCTTTC-3′
PPIA (Reverse)	5′-TTGCCACCAGTGCCATTA-3′
AABR07051515.1 (Forward)	5′-CAGCGGACAATGAGGTATGT-3′
AABR07051515.1 (Reverse)	5′-GAAGGGACCAAGGAAAGGTTAG-3′
Dio1 (Forward)	5′-CCAGAGAGAGTCAAGCAGAAC-3′
Dio1 (Reverse)	5′-ACTGGATGCTGAAGAAGGTG-3′
Gabra4 (Forward)	5′-ATGATCTACACCTGGACCAAAG-3′
Gabra4 (Reverse)	5′-CTGGATACAGTCTGGCCAATTA-3′
Htr6 (Forward)	5′-TCCTGCTGGGAATGTTCTTT-3′
Htr6 (Reverse)	5′-CCATGTGAGGACATCGAAGAG-3′
Map4k2 (Forward)	5′-ACCGCTTGTGGATATGTATGG-3′
Map4k2 (Reverse)	5′-TAGGCAATCTGCCGTTCTTC-3′
Men1 (Forward)	5′-GTACCTGGCTGGATACCATTG-3′
Men1 (Reverse)	5′-TCATCCTCCCGACAGTAGTT-3′
NMU (Forward)	5′-TTGCAGAGGTACGCCAATATC-3′
NMU (Reverse)	5′-AGACAGAAAGGACGCACAAG-3′
Orai2 (Forward)	5′-GGTAGCCGTGCACCTATTT-3′
Orai2 (Reverse)	5′-GGAGTTGAGGTTGTGGATGT-3′
Rars (Forward)	5′-GCCCAAGTTTGGAGACTATCA-3′
Rars (Reverse)	5′-TCGGCAATTTCTCTAGGACTAAC-3′
Sec1415 (Forward)	5′-CCGCTCTTTCTTTGGCTTTG-3′
Sec1415 (Reverse)	5′-GAAATGAGCTCGCTCAGATAGT-3′
Slc7a11 (Forward)	5′-CTCATTAGCAGTCCCGATCTTT-3′
Slc7a11 (Reverse)	5′-CCCTTCTCGAGATGCAACATAG-3′
AChRα3 (Forward)	5′-AAGCACAGAATGTAGCCAAAGAGA-3′
AChRα3 (Reverse)	5′-AGGATGAAAACCCAGAGAAAGATG-3′
AChRα7 (Forward)	5′-CCCAGATGTCACCTACACAGTAACC-3′
AChRα7 (Reverse)	5′-ATGAGTACACAAGGGATGAGCAGAT-3′
αSMA (Forward)	5′-GACGAAGCGCAGAGCAAGA-3′

Primers	Sequences
αSMA (Reverse)	5′-GGTGATGATGCCGTGTTCTATC-3′
β-Catenin (Forward)	5′-CCGTTCGCCTTCATTATGGA-3′
β-Catenin (Reverse)	5′-GGGCAAGGTTTCGGATCAAT-3′
Calponin (Forward)	5′-AGCGTGAGCAGGAGCTGAGAG-3′
Calponin (Reverse)	5′-GCTGGAGCTTGTTGATAAATTCGC-3′
Collagen I (Forward)	5′-CAAGATGGTGGCCGTTACTAC-3′
Collagen I (Reverse)	5′-GCTGCGGATGTTCTCAATCT-3′
Collagen III (Forward)	5′-CTGAACTCAAGAGCGGAGAATAC-3′
Collagen III (Reverse)	5′-CAGTCATGGGACTGGCATTTA-3′
Fibronectin (Forward)	5′-GTCCGAGAAGAGGTTGTTACTG-3′
Fibronectin (Reverse)	5′-GGAAACCGTGTAAGGGTCAA-3′
LEF1 (Forward)	5′-GAGCACGAACAGAGAAAGGAACA-3′
LEF1 (Reverse)	5′-TTGATAGCTGCGCTCTCCTTTA-3′
PPAR-γ (Forward)	5′-TGGCAAAGCATTTGTATGACTCA-3′
PPAR-γ (Reverse)	5′-CCTCGCCTTGGCTTTGG-3′

TABLE 2

Comparison of methylation levels across different genomic regions via Dunn test

Region 1	Region 2	*z*	*P*	P_{adj}	Sign
5′-UTR	3′-UTR	6.61949318	3.6043E-11	1.8923E-10	***
All CpGs	3′-UTR	1.94140613	0.05220904	0.06449351	+
All CpGs	5′-UTR	−4.6780871	2.8956E-06	6.7565E-06	***
Exons	3′-UTR	3.50076848	0.00046392	0.00088566	***
Exons	5′-UTR	−3.1187247	0.00181636	0.00293411	**
Exons	All CpGs	1.55936235	0.11891064	0.12485617	ns
Gene	3′-UTR	−0.7952748	0.42645367	0.42645367	ns
Gene	5′-UTR	−7.414768	1.2184E-13	8.5287E-13	***
Gene	All CpGs	−2.7366809	0.00620625	0.00868874	**
Gene	Exons	−4.2960433	1.7387E-05	3.6513E-05	***
Introns	3′-UTR	−2.7366809	0.00620625	0.00930937	**
Introns	5′-UTR	−9.3561741	8.2676E-21	1.7362E-19	***
Introns	All CpGs	−4.6780871	2.8956E-06	7.601E-06	***
Introns	Exons	−6.2374494	4.4476E-10	1.868E-09	***
Introns	Gene	−1.9414061	0.05220904	0.06852436	+
Promoter	3′-UTR	5.06013083	4.1897E-07	1.2569E-06	***
Promoter	5′-UTR	−1.5593624	0.11891064	0.13142755	ns
Promoter	All CpGs	3.1187247	0.00181636	0.00317862	**
Promoter	Exons	1.55936235	0.11891064	0.13872908	ns
Promoter	Gene	5.85540563	4.7585E-09	1.6655E-08	***
Promoter	Introns	7.79681176	6.3491E-15	6.6665E-14	***

Note: Columns: “Region 1–2” shows the genomic regions compared, “*z*” is the Dunn *z*-test statistics, “*P*” is the *P*-value, “P_{adj}” is the adjusted *P*-value, “sign” show the significance.

*** $P < .001$

** $P = .001–0.01$

* $P = .01–0.05$

+ $P = .05–0.1$

ns $p = .1–1$.